IEEE Access
Multidisciplinary : Rapid Review : Open Access Journal

Received January 20, 2019, accepted March 6, 2019, date of publication March 14, 2019, date of current version April 3, 2019.

Digital Object Identifier 10.1109/ACCESS.2019.2905000

# Electrocardiogram Reconstruction Based on Compressed Sensing

**ZHIMIN ZHANG[1,2], XINWEN LIU[2], SHOUSHUI WEI[1], HONGPING GAN[3], FEIFEI LIU[1], YUWEN LI[4], CHENGYU LIU[5], (Member, IEEE), AND FENG LIU[2]**

[1]School of Control Science and Engineering, Shandong University, Jinan 250100, China
[2]School of Information Technology and Electrical Engineering, The University of Queensland, Brisbane, QLD 4072, Australia
[3]State Key Laboratory of Integrated Services Networks, Xidian University, Xi'an 710071, China
[4]Department of Automation, Xiamen University, Xiamen 361005, China
[5]School of Instrument Science and Engineering, Southeast University, Nanjing 210096, China

Corresponding authors: Shoushui Wei (sswei@sdu.edu.cn), Chengyu Liu (chengyu@seu.edu.cn), and Feng Liu (feng@itee.uq.edu.au)

This work was supported in part by the Shandong Province Key Research and Development Plan under Grant 2018GSF118133, in part by the National Natural Science Foundation of China under Grant 81871444, in part by the Natural Science Foundation of Shandong, China, under Grant ZR2016FM11, in part by the China Scholarship Council under Grant 201706220221, and in part by the Southeast Lenovo Wearable Heart-Sleep-Emotion Intelligent Monitoring Lab.

**ABSTRACT** Compressed Sensing (CS) attempts to acquire and reconstruct a sparse signal from a sampling much below the Nyquist rate. In this paper, we proposed novel CS algorithms for reconstructing under-sampled and compressed electrocardiogram (ECG) signal. In the proposed CS-ECG scheme, the ECG signal was first sub-sampled randomly and mapped onto a two-dimensional (2D) space by using Cut and Align (CAB), for the purpose of promoting sparsity. A nonlinear optimization model was then used to reconstruct the 2D signal. In the compression scheme, the ECG signal was mapped into the frequency domain, and the compression was achieved by a series of multiplying and accumulating between the original ECG and a Gaussian random matrix. For the reconstruction, two matching pursuits (MP) methods and two blocks sparse Bayesian learning (BSBL) methods were implemented and evaluated by the percentage root-mean-square difference (PRD). Based on the test with real ECG data, it was found that the proposed CS scheme was capable of faithfully reconstructing ECG signals with only 30% acquisition.

**INDEX TERMS** Compressed sensing (CS), compression, electrocardiogram (ECG), reconstruction, subsampling.

## I. INTRODUCTION

The conventional method of 12-lead electrocardiogram (ECG) signal acquisition is widely used in most static ECG acquisition equipment for patients at rest. Nowadays, the research to dynamic ECG monitoring is very active as cardiovascular disease is a major killer worldwide [1], [2]. For example, in 2017, Apple announced a heart study program cooperated with *Stanford MEDICINE*, and one year later they have successfully realised ECG data collection and atrial fibrillation (AF) analysis in their new product. Nevertheless, the current technical developments may still behind the practical use for clinical diagnosis. One technical challenge is to perform dynamic ECG acquisition. Those conventional ECG acquisition methods cannot be used in dynamic environment because of its complex connection configuration and high energy consumption. Therefore, a novel ECG acquisition method should be designed with several features: real-time, lower power consumption, smaller size, and wireless [3], [4]. Also, ECG compression algorithms should be applied to reduce the burden of data transmission and storage. In addition, the ECG signal quality and reconstruction are of great concern about its usability for clinical diagnosis.

As a breakthrough to *Shannon's sampling theorem*, compressed sensing (CS) [5], [6] has aroused great concerns in information theory, image processing [7], microwave imaging, pattern recognition and wireless communication [8]. Recently, CS has been used in the design of ECG signal acquisition, processing and compression framework [9]. By exploiting the block structure of ECG signal in time domain and an uncorrelated domain, two CS recovery algorithms are proposed in [10]. Simulations show that the proposed scheme could reduce the compression ratio by 44%. Mamaghanian *et al.* [4] apply the CS

The associate editor coordinating the review of this manuscript and approving it for publication was Liangtian Wan.

signal acquisition/compression paradigm for low-complexity and energy-efficient signal compression of ECG data collected from a wireless body sensor network (WBSN) and results show that the CS algorithm represents a competitive alternative to state-of-the-art ECG compression solutions in WBSN-based ECG monitoring systems. In [11], several considerations including sparsity, compression limits, thresholding techniques, and signal recovery algorithms were presented. Simulation studies showed that compression factors greater than 16X are achievable for ECG signals with signal to noise ratio (SNR) greater than 60 dB. In [12], a real-time CS-based personal ECG monitoring system was proposed. Polania *et al.* [13] applied distributed CS to exploit the common support between samples of jointly sparse adjacent beats. These studies showed that CS would be very effective in ECG compression.

In this paper, we aim to present a novel CS scheme for ECG processing. The proposed CS frameworks handle ECG signal reconstruction based on both data under-sampling and compression. Our method also considers two types of correlations in ECG waveforms, including (1) intra-beat correlation and (2) inter-beat correlation. This is different from conventional CS-ECG methods that typically ignore the inter-beat correlation between adjacent heartbeats. Specifically, a two-dimensional (2D) signal model is employed to fully utilise both inter-beat correlation and intra-beat correlation to recover the under-sampled signal. While in signal compression and reconstruction, several considerations including sampling frequency, compression ratio and reconstruction time are investigated to find the best settings for the CS-based ECG data processing.

The following paragraphs are organised as follows: Section II gives the reasons why we choose CS for ECG processing. Section III elaborates the proposed CS-ECG framework. In section IV, testing results are presented. Discussions and conclusions are presented in section V and Section VI, respectively.

## II. WHY COMPRESSED SENSING

According to Shannon's sampling theorem, in order not to lose information when uniformly sampling a signal, the minimum sampling rate should be twice of the signal bandwidth [9]. To satisfy this minimum sampling rate, the transmission and storage burden would become quite large for high-frequency signals, such as images and videos. In addition, the traditional signal acquisition and compression scheme has several drawbacks: i) the signal needs to be completely sampled before compression, and ii) the compression process is realised with complex algorithms. There is an unavoidable problem that some data acquired at high computational cost would still be discarded during compression. This leads to a huge waste of resources.

In 2004, Candes, Donoho and Tao proposed compressive sensing theory that breaks the conventional procedure [6], [14], [15]. It indicates that the compressible data can be sampled and reconstructed accurately with much lower sampling rate than Nyquist rate. Different from *Shannon's sampling theorem*, CS sampling and compression are to be achieved simultaneously. Three basic requirements for CS need to be satisfied, which are incoherence, sparsity and nonlinear reconstruction [14], [16], [17]. The benefit of incoherence is that it ensures the noise-like artifacts, which can be reduced by using a filtering mechanism [17], [18]. To enhance the incoherence, random sampling is employed during the signal acquisition process. Moreover, If the original signal is sparse in some transformation domain, it can be projected to a lower dimensional observation vector [19]. Then the original signal can be reconstructed from the acquired vector by solving sparse optimisation problems. Under this theoretical framework, the required sampling frequency is determined by the sparsity of the original signal rather than its bandwidth. The CS signal acquisition requires a more complex and high-computational reconstruction process which can be achieved by more advanced computing facilities [20]. The mathematical model of CS is given in *Appendix*.

## III. PROPOSED FRAMEWORK

In this work, we propose novel CS algorithms for reconstructing under-sampled and compressed ECG signal.

### A. ECG ACQUISITION AND RECONSTRUCTION

There are two steps involved in ECG signal subsampling and reconstruction. Firstly, during the signal acquisition process, a random sampling scheme is employed to enhance the incoherence and to reduce the number of measurements significantly. Secondly, the acquired ECG signal is re-arranged into a 2D array using Cut and Align (CAB), which is used to explore signal sparsity further. At last, a nonlinear optimisation model is used to recover the original signal. The block diagram of the proposed framework is presented in Fig. 1. The framework starts with inputting an original under-sampled ECG signal and ends with outputting the reconstructed ECG signal.

#### 1) UNDER-SAMPLING PATTERN

The incoherence in CS ECG is achieved by a modified uniformly random sampling pattern. The pattern is uniformly under-sampled in the whole process and densely sampled in the QRS area. As is shown in Fig. 1 (a) and (b), a fast QRS detection method based on optimised knowledge [21] is applied on a given ECG signal to detect the R-peak. This allows us to estimate the mean heartbeat period from R-R intervals and locate the region of interest (RoI). The mask for sampling is constructed with RoI densely sampled while other areas sparsely sampled. Although this acquisition scheme leads to the artifacts noise-like, in the sparse transform domain, the significant coefficients are much larger than the noise-like interference, which can be eliminated by using noise removal algorithms.

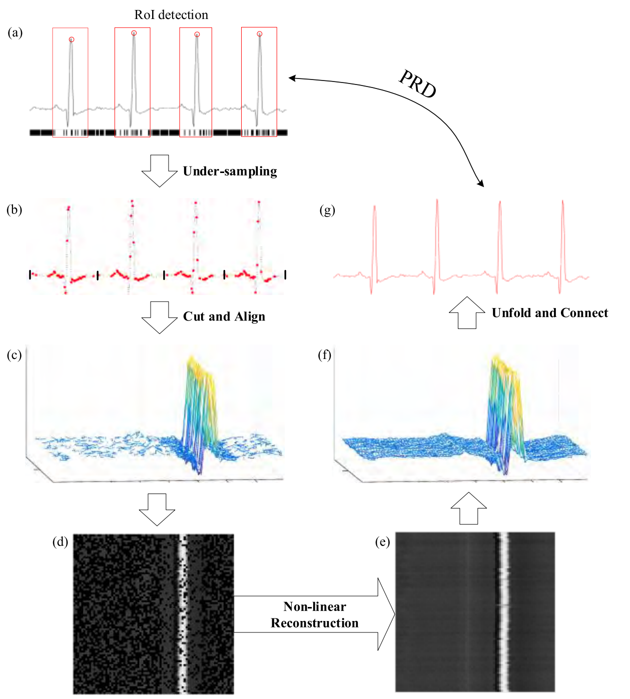


FIGURE 1. The block diagram of ECG acquisition and reconstruction in the proposed 2D scheme.

#### 2) DATA PREPROCESSING AND TRANSFORM SPARSITY

The construction of the 2D ECG array is illustrated in Fig. 1 (c) and (d). The under-sampled signal is segmented according to the heartbeat period. Since ECG signal is quasi-periodic, each R-R interval is not necessarily the same. Therefore, in order to make sure the length of each segment is uniform, an appropriate number of zeros is padded to the end of each heartbeat data sequence. Then the segmented signals are aligned according to R-peak to construct the 2D array so that the RoI of each period can be aligned in the same position of each row. As a result, the inter-beat correlation between adjacent heartbeats would be utilised in the 2D ECG reconstruction. Fig. 1 (c) is a 3D view of 2D under-sampled signal, and Fig. 1 (d) is the planform of Fig. 1 (c). The black dots in Fig. 1 (d) show the un-sampled signal while the non-black parts are the sampled. The grey scale corresponds to the intensity of each pixel, where dark represents smaller value and the bright represents larger values.

The sparsity of ECG signal can be observed in the Fourier domain as shown in Fig.2. Fig. 2 (c) is the original 2D ECG array in Fourier domain, where the principal components are concentrated only in the low frequency area. Fig. 2 (d) shows the undersampled signal in Fourier domain, where the artifacts are noise-like and far below the principal components.

#### 3) NON-LINEAR RECONSTRUCTION

After the signal being partially acquired and formulated into 2D space, we employ the non-linear signal reconstruction algorithm to reconstruct the signal. The reconstruction can

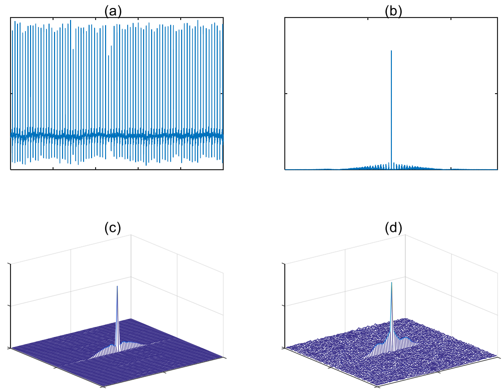


FIGURE 2. ECG signal and its sparsity in frequency domain. (a) Original ECG signal. (b) Frequency domain of (a). (c) Frequency domain of 2D ECG. (d) Frequency domain of under-sampled 2D ECG.

be modelled as the following optimisation problem:

$$minimize \; \|\psi x\|_1 \quad s.t. \; \|y - \phi x\|_2 < \epsilon \tag{1}$$

Suppose the reconstructed signal in 2D is $x$, let $y$ denote acquired under-sampled signal, $\Phi$ represent acquisition matrix, and $\Psi$ indicate the sparse transformation.

To find the solution $x$, the above optimization problem is converted to the following constrained optimization model:

$$\hat{x} = arg \min_{x} \left( \|y - \phi x\|_2^2 + \lambda \, \|\psi x\|_1 \right) \tag{2}$$

where $\|.\|_2$ denotes $l_2$-norm operation, $\|.\|_1$ denotes $l_1$-norm operation, and $\lambda$ is the regularization parameter. $l_2$-norm controls the data fidelity, and the $l_1$ norm ensures the sparsity of the signal. The conjugate gradient optimization algorithm is employed to iteratively find the solution $x$.

### B. ECG COMPRESSION AND RECONSTRUCTION

This subsection presents the ECG signal compression and reconstruction. The block diagram of the proposed framework for compressed signal reconstruction is presented in Fig. 3. The framework starts with inputting an original ECG signal and ends with outputting the reconstructed ECG signal.

#### 1) RE-SAMPLING

Zamolo [22] demonstrate that Sample Frequency (SF) is a key factor determining the performance of compression and reconstruction. In this study, we resample the signal to SFs of 260 Hz, 360 Hz, and 480 Hz respectively.

#### 2) SIGNAL COMPRESSION

In this study, we use a Gaussian random matrix [23] to acquire the compressed signal from the original ECG. The compression procedure of CS can be summarised as a series of multiplication and accumulation between ECG signal and measurement matrix [24]. The scheme of the CS compression is shown in Fig. 4. It is noted that a further mathematical illustration of Fig. 4 is given in Fig. 11 in Appendix.

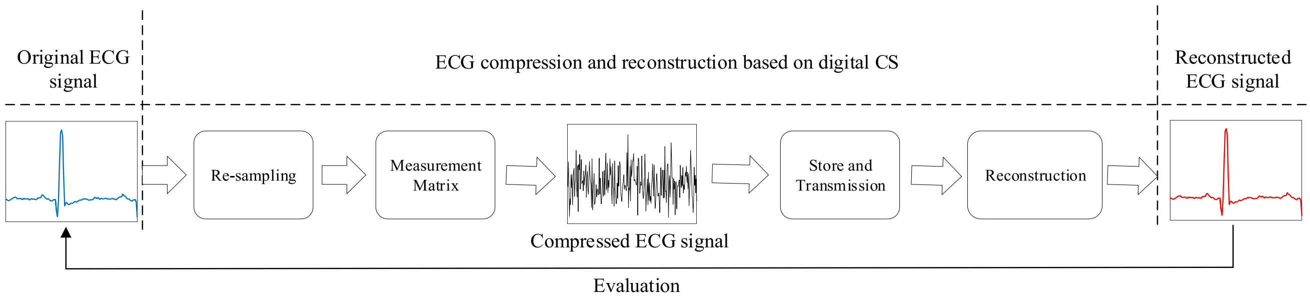


**FIGURE 3.** **The block diagram of ECG compression and reconstruction in the 1D scheme.**

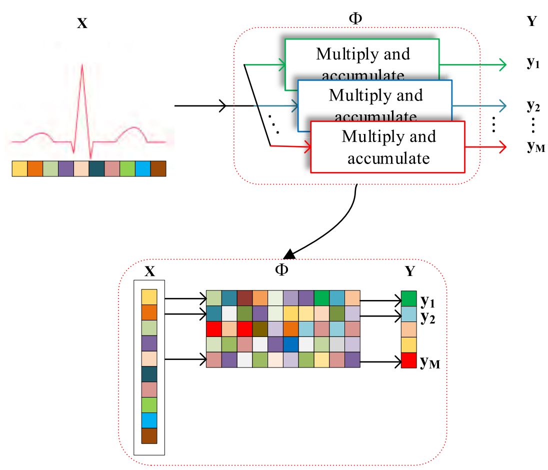


**FIGURE 4.** **The scheme of 1D CS compression. Noting that different colours in X, Φ, and Y indicate different entries.**

The reconstruction performance is highly related to Compression Ratio (CR) [22], and different CRs from 30% to 70% with a 5% step are tested to find the relationship between CR and the reconstruction performance. CR is defined as:

$$\mathrm{CR} = \frac{M}{N} \times 100\% \tag{3}$$

where M represents the length of the measurement signal and N is the length of the original ECG.

### 3) SIGNAL RECONSTRUCTION

In this paper, fully-acquired ECG signal is mapped to frequency domain as its sparse space (see Fig.2 (b)). The compressed signal is reconstructed by applying four commonly used recovery algorithms. Orthogonal Matching Pursuit (OMP) algorithm [25], [26] reconstructs the first K maximum in the frequency domain of ECG signal and acquires the reconstructed data through inverse Fourier transformation. Compressed Sampling Matching Pursuit (CoSaMP) algorithm [27], [28] applies similar principles of OMP. However, it chooses more atoms than OMP algorithm during iteration. For Bound-Optimization-based Block Sparse Bayesian Learning (BO_BSBL) and Expectation-Maximum-based Block Sparse Bayesian Learning (EM_BSBL), they both exploit the intra-block correlation in the block sparse model [29]–[31]. The ECG reconstruction is tested with real data.

The detailed program flow of real-data simulations is given in Fig. 5, and it consists of three main steps and four sub-steps. To reduce the effect of randomisation, we repeat each simulation 100 times and report the mean and standard deviation (SD) values of each performance metrics.

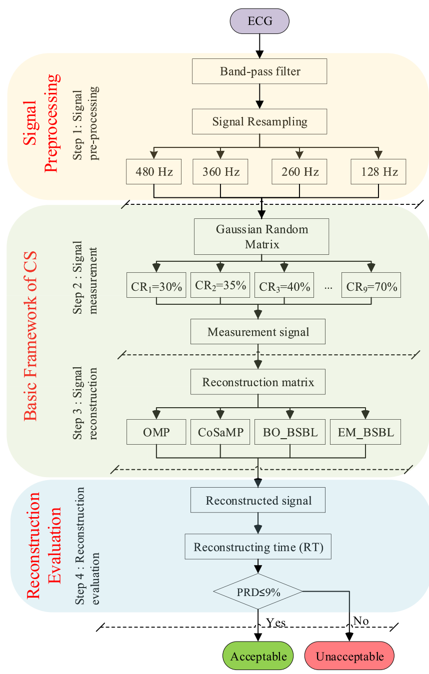


**FIGURE 5.** **Program flow of real-data simulations.**

## C. EVALUATION

Percentage of Root-mean-square Difference (PRD) [10] is commonly used to evaluate the performance of ECG reconstruction. It represents the differences between the original ECG and the reconstructed signal, and the smaller PRD value indicates the better reconstruction performance. PRD is defined as:

$$\mathrm{PRD} = \frac{\left\|\hat{x} - x\right\|_2}{\|x\|_2} \times 100\% \tag{4}$$

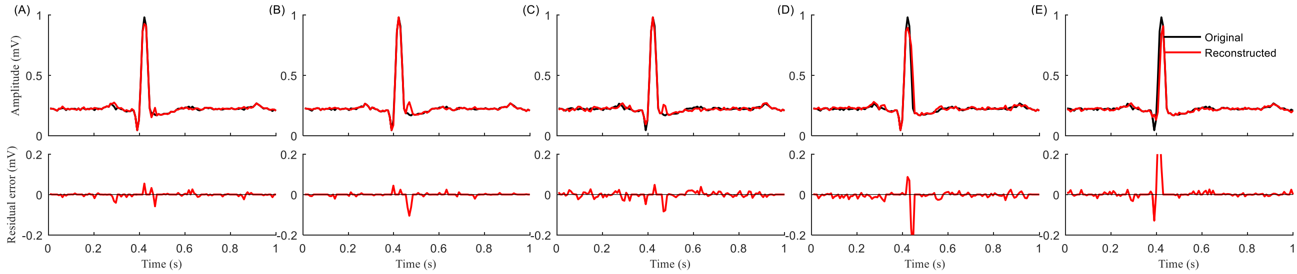


**FIGURE 6.** The under-sampled reconstruction results for '1626' with different CR: 30% (PRD=6.23%), 40% (PRD=5.62%), 50% (PRD=5.34%), 60% (PRD=4.64%), and 70% (PRD=4.33%) from left to right.

where $\hat{x}$ is the reconstructed signal, $x$ is the original ECG and $\|.\|_2$ denotes 2-norm operation. It is widely acknowledged that a reconstructed signal can be accepted only if the corresponding PRD $\leq$ 9% [10]. For ECG compression and reconstruction, the Reconstruction Time (RT) is also recorded to compare the efficiency of different reconstruction algorithms. The experiments are performed in MATLAB R2014a on a computer with 3.30G-CPU and 4.00G-RAM.

## IV. RESULTS

We use the data from MIT-BIH Normal Sinus Rhythm Database (NSRDB) of Physionet [32], in which subjects included had no significant arrhythmias. Single leads from records 16265, 16272, 16273, 16483, 16786, 17453, 18177, 18184, 19190 and 19140 are employed for the experiments in this paper. The recordings are digitized at 128 samples per second with 11-bit resolution.

### A. ECG UNDER-SAMPLING

In this subsection, we give the results for under-sampled ECG reconstruction using the proposed method.

Fig. 6 shows the overall simulation performance on 16265 from 70% to 30% acquisition. It can be seen that the reconstructed results are close to the original results, especially in the region of interest. The PRD is less than 9%, and the residual errors are quite small.

Fig.7 illustrates the simulation results on different test data with different CR, which represents the amount of data acquired. It is clear that the PRD is decreased with an increased sampling rate from 30% to 70%. All the simulated results have PRDs smaller than 9%, which means the proposed method is feasible for practical applications.

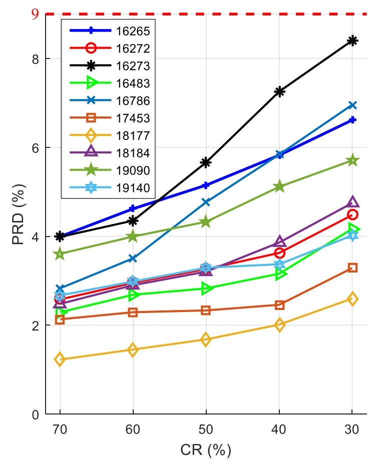


**FIGURE 7.** The under-sampled reconstruction results with different CR.

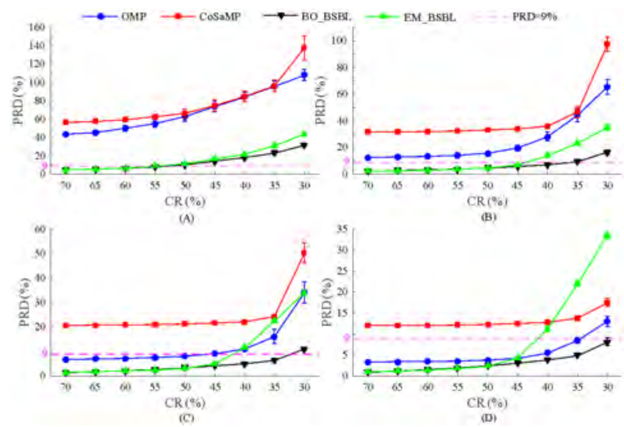


**FIGURE 8.** PRD vs. CR vs. SF for 4 recovery algorithms. (A) SF=128 Hz. (B) SF=260 Hz. (C) SF=360 Hz. (D) SF=480 Hz.

### B. ECG COMPRESSION AND RECONSTRUCTION

In the following, we present the results for ECG compression and reconstruction under different simulation settings.

#### 1) PRD vs. CR vs. SF

Fig. 8 illustrates the PRD vs. CR for four recovery algorithms at different SFs. For all the four methods, we compare the PRD when CR varies from 70% to 30% and four SF values, which are SF = 128 Hz, SF = 260 Hz, SF = 3604 Hz and SF = 480 Hz respectively. The purpose of these simulations is to define the suitable set of settings that allows achieving a smaller PRD and, on the other hand, we desire to find the best choice of recovery algorithm with the smallest CR. In subfigures (A) and (B), when SF = 128 Hz or SF = 260 Hz, it is clearly shown that the two BSBL methods outperform MP methods. The two MP methods cannot achieve a PRD less than 9% even with the highest CR = 70%. While when SF is increased to 360 Hz or 480 Hz, subfigures (C) and (D) show that the PRD of four algorithms all turns smaller.

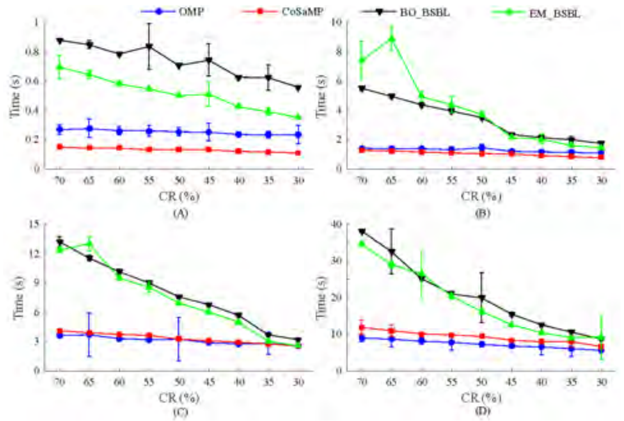

**FIGURE 9.** RT vs. CR vs. SF for 4 recovery algorithms. (A) SF=128Hz. (B) SF=260Hz. (C) SF=360Hz. (D) SF=480Hz.

Specifically, OMP could even achieve a similar performance with two BSBL methods, EM_BSBL deteriorates rapidly as CR is decreased to less than 45%, BO_BSBL still keeps good performance even with a slight increase of CR, whereas, CoSaMP is the worst one with PRD $> 9\%$ even at the highest CR $= 70\%$.

#### 2) RT vs. CR vs. SF

In order to compare the time differences for the applied algorithms, RTs are recorded for the reconstruction of a 10-s ECG signal. Similarly, Fig. 9 illustrates the RT vs. CR for four recovery algorithms at different SFs. CR is decreased from 70% to 30%, and RT is compared between different recovery algorithms and SFs. It shows that RT of both BSBL methods is always higher than that of two MP methods, and BSBL methods would perform faster at a smaller CR. Whereas, MP methods are less sensitive to CR and intend to reconstruct at stable RTs. Specifically, EM_BSBL would be slightly faster than BO_BSBL at most times, but the superiority is not obvious. It is noted that an RT $<$ 10s is accepted here because we give the results for the reconstruction of a 10-s ECG signal. In other words, the RT is accepted only when it is less than the time length of the original ECG in real-time applications.

#### 3) EVALUATION OF RECOVERY ALGORITHMS

In this section, we rank the recovery algorithms considering all the desired performance metrics, i.e., a smaller CR, a smaller SF, and an RT as smaller as possible for PRD $< 9\%$. In Table 1, we summarise the minimum CR and its corresponding RT at fixed SF for each recovery algorithm when PRD $<$ 9%. The bold in Table 1 emphasises the best choice for each fixed SF. For example, when SF $=$ 480 Hz, a CR of 30% is enough for BO_BSBL, while the minimum CR for OMP and EM_BSBL is higher to 35% and 45% respectively, whereas, a CR as high as 70% is still infeasible. Thus, the best choice when SF $=$ 480 Hz is BO_BSBL. The other three cases are also given in Table 1. It is noted that as the SF is decreased from 480 Hz to 128 Hz, the required minimum CR for each algorithm increases correspondingly, whereas RT decreases on the contrary. The last column gives the best choice of recovery algorithm for each case. It shows that BO_BSBL is always the one. Besides, it should be pointed out that we give more weights to CR than RT when considering the best recovery algorithm. That is because even the longest RT is Table 1 (*9.03s for EM_BSBL*) is still feasible for a 10-s ECG.

**TABLE 1.** The minimum CR and the corresponding RT for PRD $< 9\%$.

| SF | Algorithms | CR (%) | RT (s) | Best choice |
|---|---|---|---|---|
| 128 Hz | OMP | >70 | - | **BO_BSBL/ EM_BSBL** |
| | CoSaMP | >70 | - | |
| | **BO_BSBL** | **55** | **0.84±0.16** | |
| | **EM_BSBL** | **55** | **0.55±0.00** | |
| 260 Hz | OMP | >70 | - | **BO_BSBL** |
| | CoSaMP | >70 | - | |
| | **BO_BSBL** | **40** | **2.16±0.10** | |
| | EM_BSBL | 45 | 2.16±0.09 | |
| 360 Hz | OMP | 50 | 3.24±2.21 | **BO_BSBL** |
| | CoSaMP | >70 | - | |
| | **BO_BSBL** | **35** | **3.66±0.11** | |
| | EM_BSBL | 45 | 5.99±0.21 | |
| 480 Hz | OMP | 35 | 6.04±2.20 | **BO_BSBL** |
| | CoSaMP | >70 | - | |
| | **BO_BSBL** | **30** | **8.62±0.22** | |
| | EM_BSBL | 45 | 9.03±0.23 | |

#### 4) RECONSTRUCTION EXAMPLES

Fig. 10 shows examples of the reconstructed signal waveforms compared with the original ECG. Fig.10 (A) - (D) represent examples at different SFs respectively. In each subfigure, OMP **(top left)**, CoSaMP **(top right)**, BO_BSBL **(bottom left) and** EM_BSBL **(bottom right)** are illustrated respectively. For each algorithm, the upper one gives ECG waveforms from original and reconstructed signals while the lower one represents the residual error between them.

## V. DISCUSSIONS

### A. RECONSTRUCTION PERFORMANCE OF THE FOUR RECOVERY ALGORITHMS

Fig. 8 reveals that:

- The reconstruction PRD of the four algorithms all appears no significant signal degeneration when the original ECG is acquired at a CR higher than 50%, which means a blindly increasing CR provides no help to improve the reconstruction performance. Instead, the power consumption during data acquisition would increase. As a result, a trade-off is needed to find the best CR for the lowest power consumption.
- EM_BSBL would provide a very good reconstruction performance at a higher CR, whereas it turns deterioration rapidly as the CR is decreased lower than 45%. However, BO_BSBL appears much more stable even

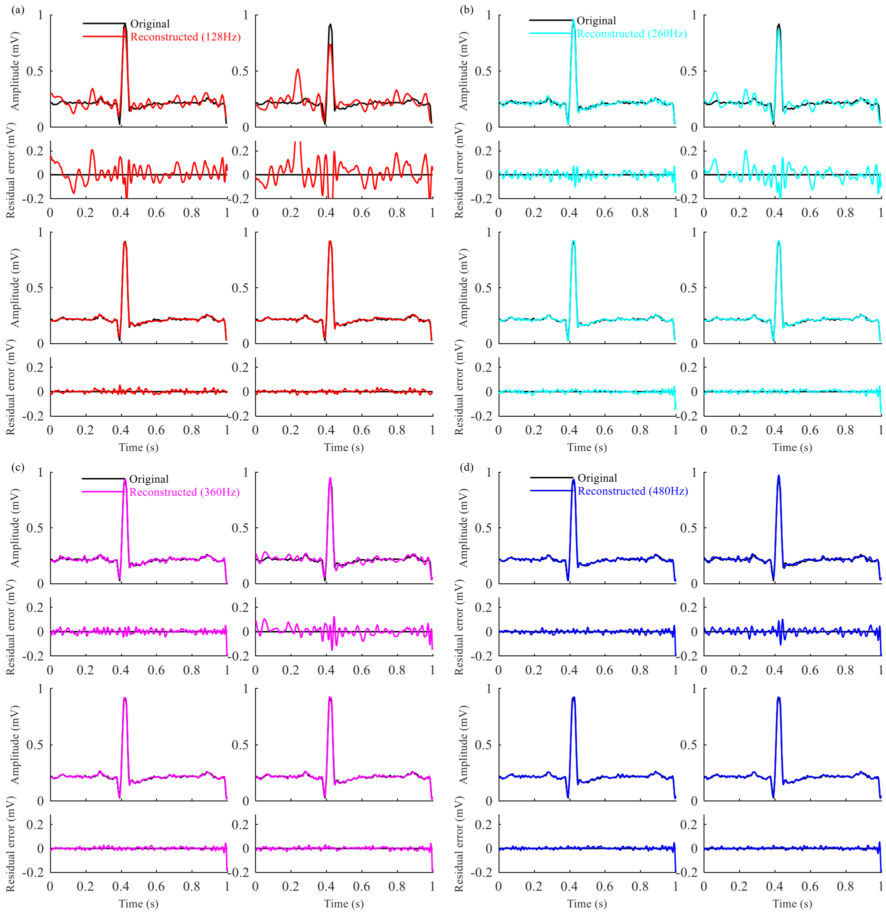


**FIGURE 10. Examples of the reconstructed ECG waveforms (1s) compared with the original signal using four different algorithms. (a) SF=128 Hz, CR=55%. (b) SF=260 Hz, CR=40%. (c) SF=360 Hz, CR=35%. (d) SF=480 Hz, CR=30%.**

with a lower CR, which is another reason why we consider BO_BSBL as the best algorithm.

- Both BSBL methods have obvious superiority to MP methods, whereas this superiority becomes smaller as the original ECG is sampled at higher SF.

At the same time, Fig. 9 reveals that:

- The needed reconstruction time of BSBL methods is much more sensitive to CR compared with MP methods. It clearly shows that the RT of BSBL methods decreases rapidly as CR turns smaller, which is because the amount of data needed to be reconstructed decreases with a smaller CR.
- It is worth noting that the RTs in Fig. 9 present the reconstruction time for a 10-s original ECG. In real-time applications, the RT is only acceptable when it is less than 10 s, which means that the reconstruction speed needs to be higher than the acquisition one.

### B. THE CHOICE OF SF

From Table 1 and Fig. 8, it is evident that the best performance, in terms of CR, is obtained when the signal is sampled at 480 Hz. However, this consideration is not entirely true because it does not take into account the final amount of data. Indeed, we focus on the low power consumption during data storage and transmission, and it is highly influenced by the total amount of acquired data. Therefore, the choice of 480 Hz may be not suitable for practical applications.

In Table 1, if we choose the BO_BSBL as the recovery algorithm, the minimum CR is 30% when the data is sampled at 480 Hz. As a result, 1440 samples need to be acquired for a 10-s ECG signal. Whereas, in the other three cases, if the original ECG is sampled at 360 Hz with a CR of 35%, 1260 samples are required; if it is sampled at 260 Hz with a CR of 40%, 1040 samples are required, while if it is sampled at 128 Hz with a CR of 55%, only 704 samples are required. Therefore, a lower SF allows acquiring a smaller amount of samples, with the acceptable PRD value, even if the CR is much higher. It also reveals that the 1D CS model does not have the requirement for a higher sampling frequency.

### C. ECG ACQUISITION AND RECONSTRUCTION

The under-sampled acquisition process utilises the QRS detection to realise modified random sampling, where QRS is densely sampled. The pattern, which acquires less data, results in a faster process and accurate reconstruction. With only 30% acquisition, the reconstruction results are accurate with PRD far less than 9%. We repeat the proposed methods on ten datasets, and the results are all promising.

In the reconstruction process, we also tried to add total variation regularisation to smooth the signal. However, the PRD has less than 5% improvement. To save the computational complexity, we discard the TV regularisation and only keep the data fidelity and sparsity control.

## VI. CONCLUSION

In this paper, we have presented novel CS algorithms for ECG reconstruction on under-sampled and compressed signals.

In the reconstruction of under-sampled acquisition, RoI, such as the QRS complex, was first detected so that it can be densely sampled. The acquired signal was formulated into 2D signal by using CAB to fully utilise both inter-beat and intra-beat correlations. The non-linear reconstruction algorithm was then utilized to obtain the reconstructed signal and results showed that this proposed framework could realise acceptable reconstruction with no more than 30% sampling. In terms of ECG compression, it was realised by a series of multiplication and accumulation between ECG signal and a Gaussian random matrix. As for the signal reconstruction, MP and BSBL methods were given the comparisons. Real-data simulations were performed in order to find the best CS settings for ECG compression, including sampling frequency, compression ratio, and recovery algorithms. Results showed that BSBL methods had better reconstruction accuracy while MP methods are very efficient in implementation. Specifically, BO_BSBL was the best choice of making a trade-off between PRD and RT.

In the near future, the proposed CS methods will be improved in terms of efficiency and accuracy, and then tested with acquired ECG data.

## APPENDIX

### THE MATHEMATICAL MODEL OF COMPRESSED SENSING

Consider a real-valued, finite-length, discrete-time, and one-dimensional signal $X = [x_1, x_2, \ldots, x_N]^T$, it can be represented with a set of orthogonal basis $\Psi = \{\varphi_i\}_{i=1}^N$:

$$X = \Psi s \tag{5}$$

where s is the projection coefficients, and it would contain the same information as X.

If X or s contains only K nonzero elements, then the signal is called K-sparse. Sparsity is the premise for the application of CS; a better choice of sparse dictionary will guarantee sufficient sparsity of the transformed coefficients.

In addition to sparsity, measurement matrix $\Phi$ for signal acquisition and an efficient recovery algorithm are another two critical aspects of the CS method.

#### 1) SIGNAL ACQUISITION

CS theory intends to acquire the general linear measurement from the original signal by constructing an $M \times N$ measurement matrix $\Phi$:

$$\Phi = \{\phi_j\}_{j=1}^M \tag{6}$$

Restricted isometry property (RIP) condition [33], [34] is required for the design of measurement matrix. It requests that for any vector $\nu$ that sharing the same K nonzero entries as s, it has:

$$(1-\varepsilon)\|\nu\|_2 \le \|\Theta\nu\|_2 \le (1+\varepsilon)\|\nu\|_2 \tag{7}$$

where $\Theta = \Phi\Psi$ and $\varepsilon \in (0, 1)$ [9]. In other words, the matrix $\Theta$ must preserve the length of $\nu$. However, RIP is difficult to demonstrate, but it can be seen from a different point of view: incoherence. An alternative approach to RIP is to guarantee that the measurement matrix $\Phi$ is incoherent [35] with the sensing matrix $\Psi$. CS sidesteps RIP by designing measurement matrix with random entries.

In our framework, the measurement matrix is built with entries $\phi_{i,j}$ from Gaussian distributions:

$$\phi_{i,j} \sim (0, \frac{1}{M}) \tag{8}$$

Then, the M linear measurement signal $Y = [y_1, y_2, \cdots, y_M]^T$ is obtained by a series of multiplying and accumulating as follows:

$$Y = \Phi X \begin{cases} y_1 = \phi_{11}x_1 + \phi_{12}x_2 + \cdots + \phi_{1N}x_N \\ y_2 = \phi_{21}x_1 + \phi_{22}x_2 + \cdots + \phi_{2N}x_N \\ \vdots \\ y_M = \phi_{M1}x_1 + \phi_{M2}x_2 + \cdots + \phi_{MN}x_N \end{cases} \tag{9}$$

Obviously, each element in Y contains the global information of X from $x_1$ to $x_N$. Therefore, Y consists of the M global measurements to the original signal. Unfortunately, the number of unknown vectors N is far more than the number of measurements M. Thus, it is an underdetermined problem to reconstruct the original signal X from Y. While CS solves this problem by transferring it to an overdetermined problem. This is where sparsity works.

Specifically, for a K-sparse signal, it has K degrees of freedom. Thus it only needs K measurements for reconstruction. Combine (5) and (9):

$$y = \Phi X = \Phi\Psi s = \Theta s$$
$$\times \begin{cases} y_1 = \theta_{1,1}s_1 + \cdots + \theta_{1,i1}s_{i1} + \cdots + \theta_{1,iK}s_{iK} + \cdots + \theta_{1,N}s_N \\ y_2 = \theta_{2,1}s_1 + \cdots + \theta_{2,i1}s_{i1} + \cdots + \theta_{2,iK}s_{iK} + \cdots + \theta_{2,N}s_N \\ \vdots \\ y_M = \theta_{M,1}s_1 + \cdots + \theta_{M,i1}s_{i1} + \cdots + \theta_{M,iK}s_{iK} + \cdots + \theta_{M,N}s_N \end{cases} \tag{10}$$

Because there are only K nonzero entries in s, i.e., $s_{i1}, s_{i2}, \ldots, s_{iK}$, (8) can be revised as follows:

$$\begin{cases} y_1 = \theta_{1,i1}s_{i1} + \theta_{1,i2}s_{i2} + \ldots \theta_{1,iK}s_{iK} \\ y_2 = \theta_{2,i1}s_{i1} + \theta_{2,i2}s_{i2} + \ldots \theta_{2,iK}s_{iK} \\ \vdots \\ y_M = \theta_{M,i1}s_{i1} + \theta_{M,i2}s_{i2} + \ldots \theta_{M,iK}s_{iK} \end{cases} \tag{11}$$

There are M equations while K (K ≪ M) unknowns in (11). This is an underdetermined problem, and there is a unique solution which is exactly the best reconstruction of the original signal.

The mathematical model of CS based acquisition can be depicted in Fig. 11 which is a further illustration of Fig. 4.

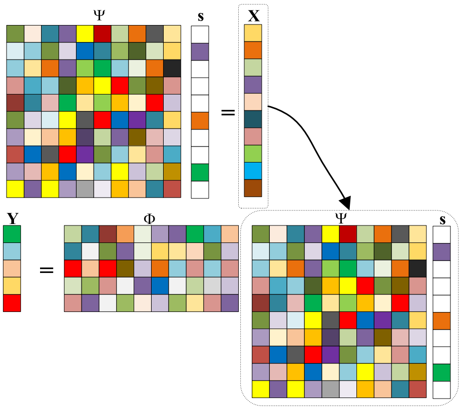


**FIGURE 11. Illustration of signal acquisition with measurement matrix Φ and sensing matrix Ψ. Noting that white indicates zero entries while colors indicate nonzero entries.**

### 2) SIGNAL RECONSTRUCTION

The detailed introduction to signal reconstruction of CS could refer to [9]. In short, recovery algorithms solve the inverse problem by applying minimum $\ell_1$ norm optimisation

$$\hat{s} = argmin \left\| s' \right\|_1 \quad \text{such that } \Theta s' = y \tag{12}$$

Here, from $M \geq CKlog(N/K)$ independent and identically distributed (*iid*) Gaussian measurements we can exactly reconstruct K-sparse vectors and closely approximate compressible vectors stably with high probability via the $l_1$ optimization.

## ACKNOWLEDGMENT

*(Zhimin Zhang and Xinwen Liu contributed equally to this work.)* The authors declare that there are no conflicts of interest to this work.

## REFERENCES

[1] Y. Wang, S. Doleschel, R. Wunderlich, and S. Heinen, "A wearable wireless ECG monitoring system with dynamic transmission power control for long-term homecare," *J. Med. Syst.*, vol. 39, no. 3, p. 35, Mar. 2015. doi: 10.1007/s10916-015-0223-5.

[2] C. Lou *et al.*, "Flexible graphene electrodes for prolonged dynamic ECG monitoring," *Sensors*, vol. 16, no. 11, pp. 1–12, 2016. doi: 10.3390/s16111833.

[3] Z. Zhang, T.-P. Jung, S. Makeig, and B. D. Rao, "Compressed sensing of EEG for wireless telemonitoring with low energy consumption and inexpensive hardware," *IEEE Trans. Biomed. Eng.*, vol. 60, no. 1, pp. 221–224, Jan. 2013. doi: 10.1109/TBME.2012.2217959.

[4] H. Mamaghanian, N. Khaled, D. Atienza, and P. Vandergheynst, "Compressed sensing for real-time energy-efficient ECG compression on wireless body sensor nodes," *IEEE Trans. Biomed. Eng.*, vol. 58, no. 9, pp. 2456–2466, Sep. 2011. doi: 10.1109/TBME.2011.2156795.

[5] E. Candes and J. Romberg, "L1-MAGIC: Recovery of sparse signals via convex programming," 2005, pp. 1–19. [Online]. Available: www.acm.caltech.edu/l1magic/downloads/l1magic.pdf

[6] D. L. Donoho, "Compressed sensing," *IEEE Trans. Inf. Theory*, vol. 52, no. 4, pp. 1289–1306, Apr. 2006. doi: 10.1109/TIT.2006.871582.

[7] J. Romberg, "Imaging via compressive sampling," *IEEE Signal Process. Mag.*, vol. 25, no. 2, pp. 14–20, Mar. 2008. doi: 10.1109/MSP.2007.914729.

[8] X. Wang, Z. Zhao, N. Zhao, and H. Zhang, "On the application of compressed sensing in communication networks," in *Proc. 5th Int. Conf. Commun. Netw. China (ICST)*, Aug. 2011, pp. 1–7.

[9] R. Baraniuk, "A lecture on compressive sensing," *IEEE Signal Process. Mag.*, vol. 24, no. 2, pp. 118–121, 2007.

[10] A. S. Lalos, L. Alonso, and C. Verikoukis, *Model Based Compressed Sensing Reconstruction Algorithms for ECG Telemonitoring in WBANs*. New York, NY, USA: Academic, 2014, pp. 105–116. doi: 10.1016/j.dsp.2014.08.007.

[11] A. M. R. Dixon, E. G. Allstot, D. Gangopadhyay, and D. J. Allstot, "Compressed sensing system considerations for ECG and EMG wireless biosensors," *IEEE Trans. Biomed. Circuits Syst.*, vol. 6, no. 2, pp. 156–166, Apr. 2012. doi: 10.1109/TBCAS.2012.2193668.

[12] K. Kanoun, H. Mamaghanian, N. Khaled, and D. Atienza, "A real-time compressed sensing-based personal electrocardiogram monitoring system," in *Proc. Design, Automat. Test Eur.*, Mar. 2011, pp. 1–6. doi: 10.1109/DATE.2011.5763140.

[13] L. F. Polania, R. E. Carrillo, M. Blanco-Velasco, and K. E. Barner, "Compressed sensing based method for ECG compression," in *Proc. IEEE Int. Conf. Acoust., Speech Signal Process.*, 2011, pp. 761–764. doi: 10.1109/ICASSP.2011.5946515.

[14] E. J. Candès, "Compressive sampling," *Proc. Int. Congr. Math.*, vol. 17, no. 2, pp. 1433–1452, 2006.

[15] R. G. Baraniuk, "Compressive sensing," in *Proc. Conf. Inf. Sci. Syst. (CISS)*, 2008, pp. 4–5. doi: 10.1109/MSP.2007.4286571.

[16] E. J. Candès, J. Romberg, and T. Tao, "Robust uncertainty principles: Exact signal reconstruction from highly incomplete frequency information," *IEEE Trans. Inf. Theory*, vol. 52, no. 2, pp. 489–509, Feb. 2006. doi: 10.1109/TIT.2005.862083.

[17] M. Lustig, D. Donoho, and J. M. Pauly, "Sparse MRI: The application of compressed sensing for rapid MR imaging," *Magn. Reson. Med.*, vol. 58, no. 6, pp. 1182–1195, 2007. doi: 10.1002/mrm.21391.

[18] M. Lustig, D. L. Donoho, J. M. Santos, and J. M. Pauly, "Compressed sensing MRI," *IEEE Signal Process. Mag.*, vol. 25, no. 2, pp. 72–82, Mar. 2008. doi: 10.1109/MSP.2007.914728.

[19] A. Marchioni, M. Mangia, F. Pareschi, R. Rovatti, and G. Setti, "Sparse sensing matrix based compressed sensing in low-power ECG sensor nodes," in *Proc. IEEE Biomed. Circuits Syst. Conf. (BioCAS)*, Oct. 2017, pp. 1–4. doi: 10.1109/BIOCAS.2017.8325155.

[20] S. Foucart and H. Rauhut, "A mathematical introduction to compressive sensing," in *Applied and Numeric Harmonic Analysis*, vol. 44. Basel, Switzerland: Birkhäuser, 2013.

[21] M. Elgendi, "Fast QRS detection with an optimized knowledge-based method: Evaluation on 11 standard ECG databases," *PLoS ONE*, vol. 8, no. 9, 2013, Art. no. e73557. doi: 10.1371/journal.pone.0073557.

[22] G. Zamolo, "Architecture design for compressed sensing-based low power systems," School Inf. Commun. Technol., Tech. Rep., 2016.

[23] K. Luo, Z. Wang, J. Li, R. Yanakieva, and A. Cuschieri, "Information-enhanced sparse binary matrix in compressed sensing for ECG," *Electron. Lett.*, vol. 50, no. 18, pp. 1271–1273, 2014. doi: 10.1049/el.2014.1749.

[24] K. Luo, Z. Cai, K. Du, F. Zou, X. Zhang, and J. Li, "A digital compressed sensing-based energy-efficient single-spot bluetooth ECG node," *J. Healthcare Eng.*, vol. 2018, Jan. 2018, Art. no. 2687389. doi: 10.1155/2018/2687389.

[25] T. T. Cai and L. Wang, "Orthogonal matching pursuit for sparse signal recovery with noise," *IEEE Trans. Inf. Theory*, vol. 57, no. 7, pp. 4680–4688, Jul. 2011. doi: 10.1109/TIT.2011.2146090.

[26] T. Y. Rezaii, S. Beheshti, M. Shamsi, and S. Eftekharifar, "ECG signal compression and denoising via optimum sparsity order selection in compressed sensing framework," *Biomed. Signal Process. Control*, vol. 41, pp. 161–171, Mar. 2018. doi: 10.1016/j.bspc.2017.11.015.

[27] M. A. Davenport, D. Needell, and M. B. Wakin, "Signal space CoSaMP for sparse recovery with redundant dictionaries," *IEEE Trans. Inf. Theory*, vol. 59, no. 10, pp. 6820–6829, Oct. 2013. doi: 10.1109/TIT.2013.2273491.

[28] B. Sathyabama, S. G. S. Sankari, and S. Nayagara, "Fusion of satellite images using Compressive Sampling Matching Pursuit (CoSaMP) method," in *Proc. 4th Nat. Conf. Comput. Vis.*, Dec. 2013, pp. 1–4. doi: 10.1109/NCVPRIPG.2013.6776256.

[29] B. Liu, Z. Zhang, H. Fan, and Q. Fu, "Fast marginalized block sparse Bayesian learning algorithm," *Comput. Sci.*, pp. 1–5, 2012. [Online]. Available: https://arxiv.org/abs/1211.4909

[30] Z. Zhang and B. D. Rao, "Sparse signal recovery with temporally correlated source vectors using sparse Bayesian learning," *IEEE J. Sel. Topics Signal Process.*, vol. 5, no. 5, pp. 912–926, Sep. 2011. doi: 10.1109/JSTSP.2011.2159773.

[31] Z. Zhang and B. D. Rao, "Extension of SBL algorithms for the recovery of block sparse signals with intra-block correlation," *IEEE Trans. Signal Process.*, vol. 61, no. 8, pp. 2009–2015, Apr. 2013. doi: 10.1109/TSP.2013.2241055.

[32] A. L. Goldberger *et al.*, "PhysioBank, PhysioToolkit, and PhysioNet: Components of a new research resource for complex physiologic signals," *Circulation*, vol. 101, no. 23, p. E215, 2000. doi: 10.1161/01.CIR.101.23.e215.

[33] R. Baraniuk, M. Davenport, R. DeVore, and M. Wakin, "The Johnson-lindenstrauss lemma meets compressed sensing," *IEEE Trans. Inf. Theory*, vol. 52, no. 3, pp. 1289–1306, 2006.

[34] E. J. Candès, "The restricted isometry property and its implications for compressed sensing," *Comp. Rendus Math.*, vol. 346, nos. 9–10, pp. 589–592, May 2008.

[35] S. Abhishek, S. Veni, and K. A. Narayanankutty, "A trick to improve PRD during compressed sensing ECG reconstruction," in *Proc. Int. Conf. Signal Process. Integr. Netw.*, Feb. 2015, pp. 174–179. doi: 10.1109/SPIN.2015.7095319.

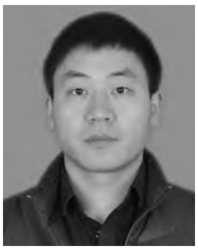

**ZHIMIN ZHANG** received the B.E. degree in biomedical engineering from Shandong University, Jinan, China, in 2014. Since then, he continued his pursuit for the Ph.D. degree with Shandong University. He is currently a research student with the School of Information Technology and Electrical Engineering, The University of Queensland, where he is mainly working on ECG, EEG signals for cardiovascular disease and sleep stages classification using compressed sensing, machine learning, and entropy analysis techniques.

**XINWEN LIU** received the bachelor's degree in engineering from the University of Science and Technology Beijing, in 2015, and the master's degree in engineering from The University of Queensland, in 2017, where she is currently pursuing the Ph.D. degree in biomedical engineering. Her research interests lie in signal processing, compressed sensing, deep learning, and MRI acceleration.

**SHOUSHUI WEI** received the M.S. degree from the Nanjing University of Aeronautics and Astronautics, Nanjing, China, in 1992. He is currently a Professor with the Institute of Biomedical Engineering, Shandong University, China. His research topics include mHealth and intelligent monitoring, machine learning and big data processing for physiological signals, early detection of CADs, device development for CADs, and sleep and emotion monitoring.

**HONGPING GAN** received the M.S. degree from Sichuan University, in 2014. He is currently pursuing the Ph.D. degree in communication and information engineering from the State Key Laboratory of ISN, Xidian University, Xi'an, China. From 2014 to 2017, he was a Research Assistant with the Chongqing University of Arts and Science, Chongqing, China. His research interests include wireless sensing networks, optimization method, sparse signal processing, and chaotic compressed sensing.

**FEIFEI LIU** received the B.S. and Ph.D. degrees in biomedical engineering from Shandong University, China, in 2010 and 2015, respectively. She has completed the postdoctoral trainings with Shandong University (2015–2017). She is currently holding the postdoctoral position with Southeast University, Nanjing, China. She has published eight original journal/conference papers. Her research topics include mHealth and intelligent monitoring, machine learning and big data processing for physiological signals, early detection of CADs, and device development for CADs.

**YUWEN LI** is currently pursuing the Ph.D. degree with the Department of Automation, Xiamen University. She is currently a joint training student with the School of Information Technology and Electrical Engineering, The University of Queensland. Her research interests include data mining and granular computing.

**CHENGYU LIU** received the B.S. and Ph.D. degrees in biomedical engineering from Shandong University, China, in 2005 and 2010, respectively.

He has completed the pngs with Shandong University, China (2010–2013); Newcastle University, U.K. (2013–2014); and Emory University, Atlanta, GA, USA (2015–2017). He is currently a Professor with Southeast University, Nanjing, China. He is currently the Director and a Professor with the Southeast-Lenovo Wearable Heart-Sleep-Emotion Intelligent Monitoring Laboratory, School of Instrument Science and Engineering, Southeast University. He was the PI on over 10 awarded grants, attracting a total of over 1 million. He has published more than 120 original journal/conference papers, eight chapters in Books, 14 Chinese invention patents, and one PCT international patent.

**FENG LIU** received the Ph.D. degree in biomedical engineering from Zhejiang University, China, in 2000. He joined The University of Queensland, in 2000. His expertise lies in medical imaging. His primary contribution has been in the areas of (1) MRI hardware design and electromagnetic analysis; and (2) cardiac electrical function imaging. He has over 260 publications to date, including over 100 fully refereed journal papers and seven patents (three of them have been licensed to the MRI industry). He is also heavily involved in collaborative and consulting projects with industry partners around the world.